Secondary structure and thermal stability of the extrinsic 23 kDa protein of photosystem II studied by Fourier transform infrared spectroscopy

Haoming Zhang[a], Yasuo Ishikawa[b], Yasusi Yamamoto[b], Robert Carpentier[a,*]

[a] *Groupe de Recherche en Energie et Information Biomoléculaires, Université du Québec à Trois-Rivières, C.P. 500, Trois-Rivières, Qué. G9A 5H7, Canada*

[b] *Department of Biology, Faculty of Science, Okayama University, Okayama 700, Japan*

Received 10 March 1998

Abstract The secondary structure and thermal stability of the extrinsic 23 kDa protein (OEC23) of spinach photosystem II have been characterized in solution between 25 and 75°C using Fourier transform infrared spectroscopy. Quantitative analysis of the amide I band (1700–1600 cm^{-1}) shows that OEC23 contains 5% α-helix, 37% β-sheet, 24% turn, and 34% disorder structures at 25°C. No appreciable conformational changes occur below 45°C. At elevated temperatures, the β-sheet structure is unfolded into the disorder structure with a major conformational transition occurring at 55°C. Implications of these results for the functions of OEC23 in photosystem II are discussed.

Key words: Extrinsic protein; Fourier transform infrared; Oxygen evolving complex 23; Photosystem II; Secondary structure

1. Introduction

On the lumenal side of photosystem II (PSII) of green plants there exist three extrinsic proteins having apparent molecular masses of 33, 23 and 16 kDa (denoted OEC33, OEC23, and OEC16, respectively). The molecular properties and physiological functions of these OEC subunits have been the subject of intensive studies since their first purification from spinach PSII [1]. As known, OEC33, OEC23 and OEC16 are all nuclear-encoded proteins and consist of 247, 186 and 149 amino acid residues, respectively [2,3]. In close association with the oxygen evolving complex, these OEC subunits are required for the maximal oxygen evolution activity of PSII (for a recent review, see [4]). In particular, the OEC33 subunit is known to stabilize the catalytic Mn cluster essential for water oxidation as release of the OEC33 leads to paramagnetic uncoupling and dissociation of two of the four Mn from PSII unless a high Cl^- concentration (>100 mM) is present [5,6]. Release of the OEC23 and OEC16 by concentrated NaCl (1–2 M) treatment partially inactivates the oxygen evolution process. Nevertheless, the oxygen evolving capacity can be restored by rebinding of the OEC23 and OEC16 through reconstitution or by addition of millimolar $CaCl_2$ [7–10]. Therefore, the OEC23 and OEC16 are thought to modulate the Ca^{2+} and Cl^- requirements in perturbed PSII. Inactivation of the OEC23 gene in a nuclear mutant of *Chlamydomonas reinhardtii* led to inhibition of the oxygen evolving activity, even though the accumulation of other subunits of PSII was not affected [11]. A more recent study showed that a similar *C. reinhardtii* mutant has low capacity to perform photoactivation and is quite sensitive to photoinhibition [12]. Although a considerable body of literature has been accumulated on the functional and biochemical aspects of OEC23, little is known about its structural organization that could provide us with information for understanding its physiological function(s). Fourier transform infrared (FTIR) spectroscopy is an established technique for probing protein secondary structure and has been increasingly applied to many water soluble as well as membrane proteins (for details, see reviews [13–15]). By this technique, secondary structural studies can be performed in solution at various physiological temperatures and pHs with minimal sample preparation, which is not accessible to other techniques such as X-ray crystallography and nuclear magnetic resonance. In the case of PSII, FTIR spectroscopy has been used to characterize the secondary structure of various PSII preparations [16–18] and isolated OEC33 [19,20]. However, the secondary structure of OEC23 has not been reported so far. In this communication, the secondary structure and thermal stability of OEC23 have been investigated in solution by means of FTIR spectroscopy and the implications of the results obtained are discussed.

2. Materials and methods

OEC23 and OEC16 were isolated from spinach PSII-enriched membranes using ion-exchange chromatography as described earlier [21]. The purities of the isolated protein samples were demonstrated as single bands on the SDS/urea-polyacrylamide gels as shown in Fig. 1. Infrared spectra were recorded at 2 cm^{-1} resolution using a Perkin-Elmer FTIR spectrometer equipped with a liquid nitrogen-cooled MCT detector. The sample compartment was continuously purged with dry air to eliminate the absorption by vapor. Lyophilized protein samples were dissolved in D_2O buffer medium (10 mM phosphate, pD 6.3) at a final concentration of ~10 mg/ml. Prior to FTIR measurements, the samples were incubated for 15 h to achieve H/D exchange. 25 μl of deuterated protein samples were loaded between CaF_2 windows with a 50 μm Teflon spacer (Harrick Scientific, New York). Each spectrum was averaged over 500 scans to obtain spectra of high quality. The temperature of the IR cell was controlled by use of an Omega CN3201 temperature controller (SpectraTech, CT). For thermal stability measurements, spectra were measured between 25 and 75°C at an interval of 5°C after 5 min of thermal equilibrium. Background spectra were measured under the identical experimental conditions as those of the protein samples and were subtracted from the sample spectra. Spectral deconvolution and curve fitting were performed as described in [19], while SDS/urea-polyacrylamide gel electrophoresis and measurements of oxygen evolution were carried out as described in [22].

*Corresponding author. Fax: (1) (819) 3765057.
E-mail: Robert_Carpentier@UQTR.Uquebec.CA

Abbreviations: FTIR, Fourier transform infrared; OEC, oxygen evolving complex; PSII, photosystem II; SDS, sodium dodecyl sulfate

PII S0014-5793(98)00371-8

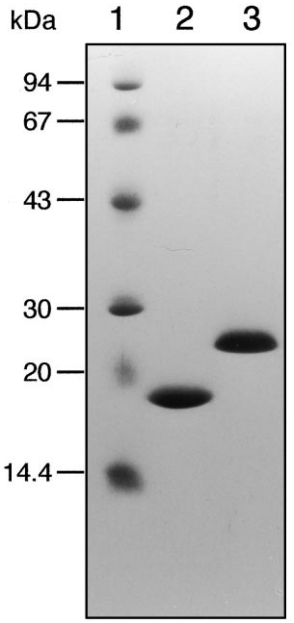

Fig. 1. SDS/urea-polyacrylamide gel patterns of the isolated OEC23 and OEC16. Lane 1, protein standards; lane 2, OEC16; lane 3, OEC23. 25 μg of OEC16 and OEC23 samples were loaded in the gels.

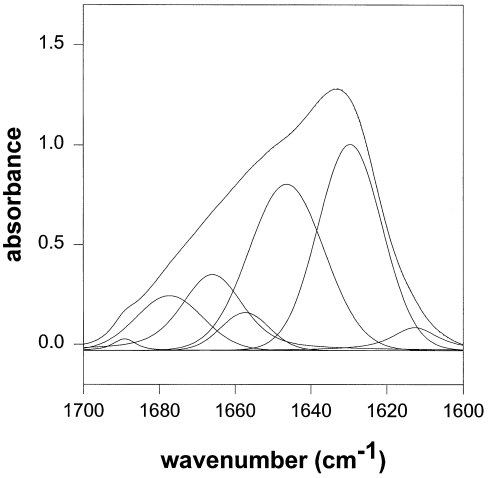

Fig. 2. Infrared absorption, curve fitted and deconvoluted spectra of OEC23 in the amide I band region at 25°C. Solid line, absorption and deconvoluted spectra; dotted line, curve fitted spectrum.

3. Results

3.1. Reconstitution of PSII with the isolated OEC23 and OEC16

Reconstitution experiments were performed to examine the quality of the isolated OEC subunits and to ensure subsequent FTIR measurements reflect the properties of OEC23 in native state. The rates of oxygen evolution in the control, NaCl-treated, and polypeptide-reconstituted PSII-enriched membrane samples are presented in Table 1. As expected, 1 M NaCl treatment resulted in inhibition of oxygen evolution to 29% of the control due to dissociation of OEC23 and OEC16 by NaCl treatment and the inhibited rate was restored to 73% by addition of 20 mM $CaCl_2$. It is notable that reconstitution of the NaCl-treated PSII-enriched membranes with the isolated OEC23 and OEC16 restored the rate of oxygen evolution up to 92% without the addition of $CaCl_2$, and the reconstituted PSII-enriched membranes do not show significant Ca^{2+} and Cl^- requirements for oxygen evolution. The recovery of the oxygen evolving activity in the NaCl-treated PSII-enriched membrane by reconstitution indicates that the isolated OEC23 and OEC16 are not irreversibly damaged during sample preparation. It is noteworthy that deuteration has no detrimental effect on OEC23 and OEC16 as the NaCl-treated PSII-enriched membranes were reconstituted using the deuterated OEC16 and OEC23 samples.

3.2. Analysis of the secondary structure of OEC23

Fig. 2 shows the absorption, deconvoluted, and curve fitted spectra of OEC23 at 25°C in the region of the amide I band. As shown, seven constituent components are resolved under the broad contour of the amide I band using Fourier self-deconvolution [23]. The peak positions and the relative areas of the constituent components are presented in Table 2. The prominent feature of the deconvoluted amide I band is a large component at 1630 cm^{-1}, which consists of over 34% of the overall area of the amide I band. To obtain quantitative data on the secondary structure, band assignment of the constituents to specific structural domains is required so that the percentages of the secondary structures can be calculated as ratios of the area of the constituents to the overall area of the amide I band. At the current state of the art, there is no generally valid criterion that can be applied for all proteins with respect to band assignments. Despite this difficulty, a number of empirical rules are still useful [13–15,24]. It is known that most proteins enriched in β-sheet structure have absorptions between 1440 and 1420 cm^{-1} and the frequency for antiparallel β-sheet structure is about 50–70 cm^{-1} higher,

Table 1
Steady-state rates of oxygen evolution in the PSII-enriched membranes reconstituted with OEC23 and OEC16

PSII sample	Rate of oxygen evolution (μmol/mg Chl/h)[a]	
	no addition	plus 20 mM $CaCl_2$
Control	460 (100)	478 (104)
NaCl-treated[b]	133 (29)	335 (73)
Reconstituted with OEC23 and OEC16[c]	409 (92)	437 (95)

[a]The values in parentheses are percentages.
[b]1 M NaCl was used to remove OEC23 and OEC16.
[c]Reconstitution of OEC23 and OEC16 to the NaCl-treated PSII samples was carried out in a buffer medium containing 0.4 M sucrose, 40 mM MES and 5 mM NaCl (pH 6.5). Aliquots of deuterated OEC23 and OEC16 stock solutions were added to the suspension of the NaCl-treated PSII sample followed by 1 h incubation in darkness. The ratio of OEC23 and OEC16 to PSII was 3:1. Excess OEC23 and OEC16 were removed by centrifugation before measurements of rates of oxygen evolution.

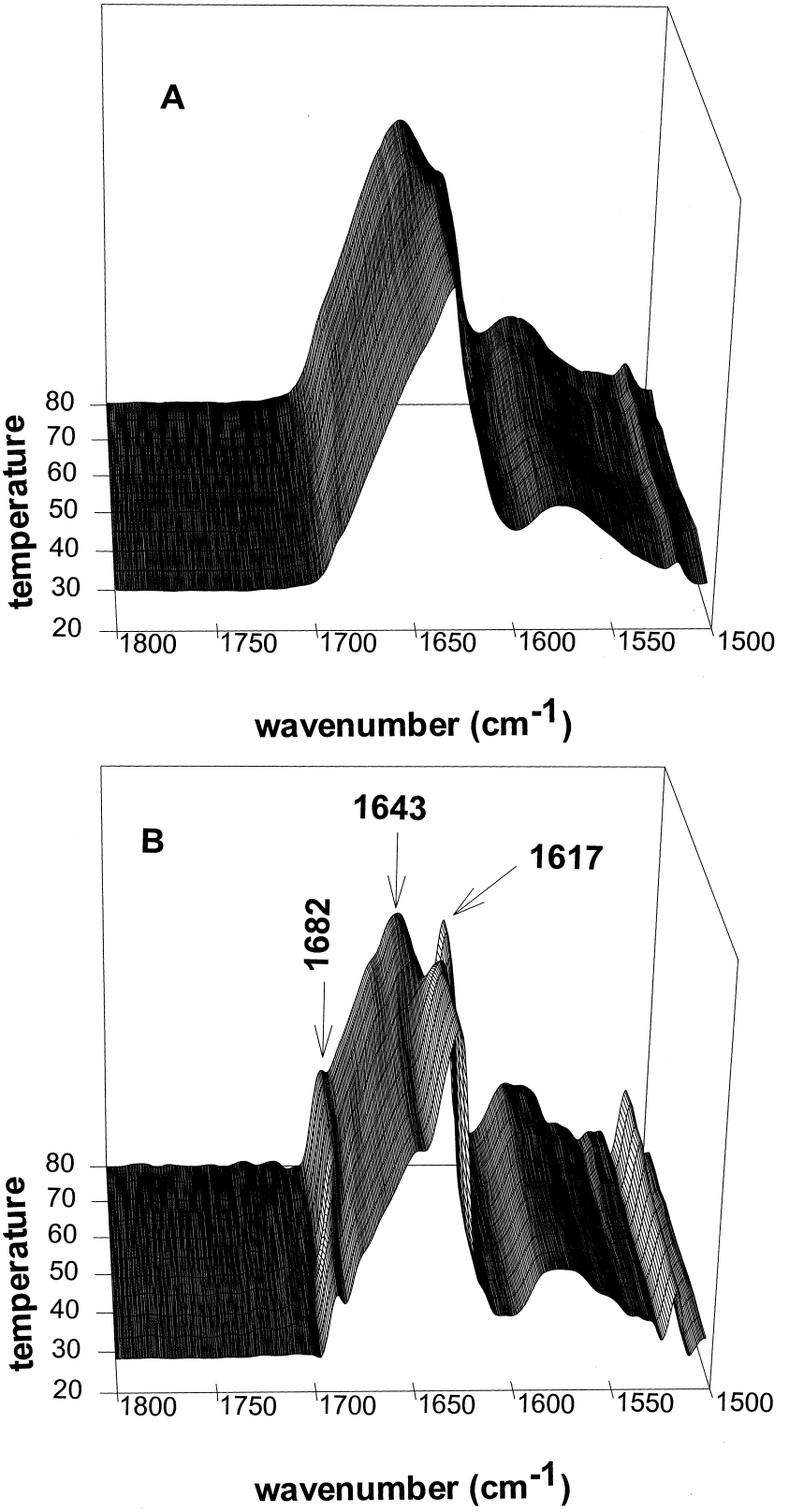

Fig. 3. Infrared absorption (A) and deconvoluted (B) spectra of OEC23 measured at various temperatures. The absorption spectra were deconvoluted with a bandwidth of 13 cm^{-1} and K=1.8.

while α-helical structure absorbs between 1660 and 1648 cm^{-1}. IR bands at 1646–1640 cm^{-1} in D_2O medium are attributed to disorder structure. Thus, the component at 1630 cm^{-1} in Fig. 2 is assigned to the β-sheet structure and the high frequency component at 1689 cm^{-1} is assigned to antiparallel β-sheet structure. The component at 1657 cm^{-1}

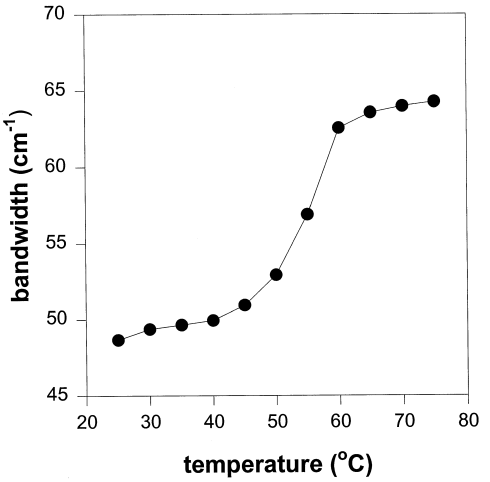

Fig. 4. Thermal profile of the bandwidth of the amide I band of OEC23 between 25 and 75°C. The bandwidth was determined at half height of the maximum peak between 1700 and 1600 cm^{-1}.

is typical of α-helical structure. Band assignments regarding other components are summarized in Table 2. It is of note that the frequency of the 1613 cm^{-1} component is too low to be assigned to any secondary structures. Most likely, this band arises from protein side chains. Thus, its contribution is not included in calculation of the secondary structure of OEC23. Based on the above assignments, the secondary structure of OEC23 is calculated to be 5% α-helix, 37% β-sheet including antiparallel β-sheet, 24% turn, and 34% disorder structures.

3.3. Thermal stability

Measurement of gradual thermal denaturation of proteins is a sensitive tool to reveal conformational changes and transitions. The temperature dependence of the amide I band of OEC23 is shown in Fig. 3. No major spectral changes in the amide I band are observed below 45°C. However, the peak position of the amide I band is clearly upshifted and a shoulder band appears in the low frequency region at increased temperatures. These features are explicitly demonstrated in the deconvoluted spectra (Fig. 3B). At 25°C, the seven constituent components in the amide I band are observed, particularly a band at 1630 cm^{-1}. At increased temperatures (> 60°C), the intensity of the 1630 cm^{-1} band attributed to the β-sheet structure is largely reduced with concomitant appearance of new bands at 1682, 1617, and 1643 cm^{-1}. The first two bands are normally associated with irreversible aggregation of proteins [25–27], while the band at 1643 cm^{-1} can be attributed to the disorder structures [24]. Thus, thermal denaturation of OEC23 is characterized by irreversible aggregation and unfolding of the orderly β-sheet structure into the disorder structure.

The bandwidth of the amide I band may be useful for identification of the temperature at which major conformational transition occurs as demonstrated in previous studies on thermal profiles of cytochrome *c* oxidase [27] and the PSII reaction center (RC) [17]. Fig. 4 shows the thermal profile of the amide I band of OEC23. Similar to that of the PSII RCs, the thermal profile of OEC23 shows a sigmoidal feature. Between 25 and 45°C, the bandwidth is only slightly increased with temperature. However, a rapid increase in the bandwidth is observed between 50 and 60°C. Thus, the major conformational transition induced by heat likely occurs at 55°C.

4. Discussion

Using FTIR spectroscopy, we have obtained the secondary structure of OEC23 as summarized in Table 2. An interesting feature of its structure is that OEC23 contains a large proportion of extended sheet structure (37%), but only 5% α-helical structure. This structural feature is in clear contrast to the secondary structure of the PSII RCs which have high content of α-helical structure (40–62%) as also determined by FTIR spectroscopy [16,17]. The high α-helical structure is considered experimental evidence supporting that the RC binding proteins of D1 and D2 have a few transmembrane α-helices. The dominating β-sheet structure of OEC23 may also be a consequence of its unique role in regulation and protection of PSII.

In current concepts, OEC23 is not essential for the oxygen evolving activity of PSII as the OEC23-less PSII still evolves oxygen although at low rates. As mentioned in Section 1, however, OEC23 is required for maximal oxygen evolution. Moreover, removal of OEC23 exposes the catalytic Mn to chemical attack by exogenous reductants such as hydroxylamine, hydroquinone, and hydrogen peroxide. Over-reduction of the catalytic Mn by these exogenous reductants leads to the release of the Mn atoms from their binding sites and consequently impairs the oxygen evolving capacity completely [28,29]. The chemical reaction between the catalytic Mn and exogenous reductants does not occur in intact PSII membranes. Since OEC23 does not provide specific binding site(s) for the Mn atoms, a structural role of OEC23 has been proposed in optimizing and shielding the structural organization of PSII on the lumenal side [8,28]. An extended sheet structure of OEC23 determined in this study is in favor of such a role because a large proportion of β-sheet structure likely facilitates more extensive interfacial contact between the OEC23 and the lumenal side of the PSII membranes. The relatively extensive contact may benefit in two ways. Firstly, it may enhance the electrostatic binding of the OEC23. The specific

Table 2
Peak positions and relative areas of the constituents of the amide I band and the quantified secondary structure of OEC23

Peak position (cm^{-1})	Area (%)	Assignment	Secondary structure	
1689	0.82	β-sheet		
1677	0.82	turn	α-helix	5%
1666	13.98	turn	β-sheet	37%
1657	4.84	α-helix	turns	24%
1646	32.76	disorder	disorder	34%
1630	34.74	β-sheet		
1613	3.29			

binding site(s) for OEC23 remains unclear although it may interact with intrinsic subunits of PSII such as CP43, a chlorophyll *a*-binding protein [30]. However, it is clear that the binding of OEC23 is mainly electrostatic as this protein can be removed by concentrated NaCl and can rebind to the PSII membrane in low salt medium. The extended sheet structure of OEC23 likely allows surface charged residues to have stronger interaction and hence increases the binding affinity. Secondly, it may restrict the accessibility of exogenous reductants to the catalytic site through a shielding effect. As mentioned earlier, chemical attack of the catalytic Mn by exogenous reductants is not possible unless the OEC23 is removed [28,31]. Moreover, removal of the OEC23 also increases the accessibility of water molecules to the catalytic site, which leads to the formation of hydrogen peroxide at the cost of lowering the oxygen evolving activity [32]. A recent structural study of PSII at low resolution showed that the removal of the OEC subunits leads to a cavity on the lumenal side of the PSII membrane [33], which is in favor of a shielding function.

Another interesting feature of the OEC23 is the thermal stability. Compared to the PSII RCs, OEC23 is more tolerant to thermal denaturation. As reported previously [17], the conformational transition temperature of the PSII RCs is 42°C, while the transition temperature of OEC23 is about 13°C higher (Fig. 4). The greater tolerance of OEC23 to thermal denaturation indicates that OEC23 may have a protective role in stabilizing the whole PSII complex under physiological stress conditions in vivo. Further experiments are required to examine such a role.

In conclusion, we have used FTIR spectroscopy to characterize the secondary structure and thermal stability of the OEC23. Analysis of the amide I band reveals that the secondary structure of OEC23 is mainly β-sheet (37%) with little α-helix (5%). This structural feature may account for the regulation and protection role of OEC23 in PSII.

Acknowledgements: The authors are grateful to NSERC (National Sciences and Engineering Research Council of Canada) for financial support.

References

[1] Yamamoto, Y., Shimada, S. and Nishimura, M. (1983) FEBS Lett. 151, 49–53.
[2] Jansen, T., Rother, C., Steppuhn, J., Reinke, H., Beyreuther, K., Jansson, C., Andersson, B. and Herrmann, R.G. (1987) FEBS Lett. 216, 234–240.
[3] Oh-Oka, H., Tanaka, S., Wada, K., Kuwabara, T. and Murata, N. (1986) FEBS Lett. 197, 63–66.
[4] Seidler, A. (1996) Biochim. Biophys. Acta 1277, 35–60.
[5] Miyao, M. and Murata, N. (1984) FEBS Lett. 170, 350–354.
[6] Murata, N. and Miyao, M. (1985) Trends Biochem. Sci. 10, 122–124.
[7] Kuwabara, T., Murata, T., Miyao, M. and Murata, N. (1986) Biochim. Biophys. Acta 850, 146–155.
[8] Åkerlund, H.-E., Jansson, C. and Andersson, B. (1982) Biochim. Biophys. Acta 681, 1–10.
[9] Ghanotakis, D.F., Babcock, G.T. and Yocum, C.F. (1984) FEBS Lett. 167, 127–130.
[10] Critchley, C., Andersson, B., Ryrie, I.J. and Anderson, J.M. (1984) Biochim. Biophys. Acta 767, 532–539.
[11] Mayfield, S.P., Rahire, M., Frank, G., Zuber, H. and Rochaix, J.-D. (1987) Proc. Natl. Acad. Sci. USA 84, 749–753.
[12] Rova, E.M., Ewen, B.M., Fredriksson, P.-O. and Styring, S. (1996) J. Biol. Chem. 271, 28918–28924.
[13] Jackson, M. and Mantsch, H.H. (1995) Crit. Rev. Biochem. Mol. Biol. 30, 95–120.
[14] Arrondo, J.L.R., Muga, A., Castresana, J. and Goni, F.M. (1993) Prog. Biophys. Mol. Biol. 59, 23–56.
[15] Surewicz, W.K. and Mantsch, H.H. (1988) Biochim. Biophys. Acta 952, 115–130.
[16] He, W.Z., Newell, W.R., Haris, P.I., Chapman, D. and Barber, J. (1991) Biochemistry 30, 4552–4559.
[17] De Las Rivas, J. and Barber, J. (1997) Biochemistry 36, 8897–8903.
[18] Zhang, H., Yamamoto, Y., Ishikawa, Y., Zhang, W., Fischer, G. and Wydrzynski, T. (1997) Photosynth. Res. 52, 215–223.
[19] Ahmed, A., Tajmir-Riahi, H.A. and Carpentier, R. (1995) FEBS Lett. 363, 65–68.
[20] Sonoyama, M., Motoki, A., Okamoto, G., Hirano, M., Ishida, H. and Katoh, S. (1996) Biochim. Biophys. Acta 1297, 167–170.
[21] Miyao, M. and Murata, N. (1983) Biochim. Biophys. Acta 723, 87–93.
[22] Bernier, M. and Carpentier, R. (1995) FEBS Lett. 360, 251–254.
[23] Kauppinen, J.K., Moffatt, D.J., Mantsch, H.H. and Cameron, D.G. (1981) Appl. Spectrosc. 35, 271–276.
[24] Byler, M.D. and Susi, H. (1986) Biopolymers 25, 469–487.
[25] Jackson, M., Haris, P.I. and Chapman, D. (1991) Biochemistry 30, 9681–9686.
[26] Surewicz, W.K., Leddy, J.J. and Mantsch, H.H. (1990) Biochemistry 29, 8106–8111.
[27] Arrondo, J.L.R., Castresana, J., Valpuesta, J.M. and Goni, F.M. (1994) Biochemistry 33, 11650–11655.
[28] Ghanotakis, D.F., Topper, J.N. and Yocum, C.F. (1984) Biochim. Biophys. Acta 767, 524–531.
[29] Tamura, N., Inoue, H. and Inoue, Y. (1990) Plant Cell Physiol. 31, 469–477.
[30] De Vitry, C., Olive, J., Drapier, D., Recouvreur, M. and Wollman, F.A. (1989) J. Cell. Biol. 109, 991–1006.
[31] Rashid, A. and Carpentier, R. (1989) FEBS Lett. 258, 331–334.
[32] Wydrzynski, T., Hiller, W. and Messinger, J. (1996) Physiol. Plant. 96, 342–350.
[33] Ford, R.C., Rosenberg, M.F., Sheperd, F.H., McPhie, P. and Holzenburg, A. (1995) Micron 26, 133–140.